

# Synthesis and spark plasma sintering of TaC-TaB<sub>2</sub> nano composites

B. MEHDIKHAN<sup>a, b\*</sup>, S. R. BAKHSHI<sup>b</sup>

<sup>a</sup>Department of Materials Engineering, Malek-e-ashtar University of Technology, Isfahan, Iran

<sup>b</sup> Construction and Mining Department, Standard Research Institute, Karaj, Iran

In this study, mechanochemical process (MCP) is applied to synthesize ultrafine TaC powders. In this research, nano powder composite TaC-TaB<sub>2</sub> was produced using mixtures of tantalum carbide and boron carbide as raw materials via mechanochemical process. Using fine tantalum carbide/boride composite (TaC-TaB<sub>2</sub>) powder, monolithic TaC-TaB<sub>2</sub> ceramics with a relative density of 85% was obtained by spark plasma sintering (SPS) at 1900°C and 30 Mpa pressure for 10 min. It is considered that the small particle size of TaC-TaB<sub>2</sub> powder is an important factor for preparing dense TaC-TaB<sub>2</sub> ceramics with fine microstructure. The phase formation characterization during synthesis process of powders and sintered samples were utilized by X-ray diffractometry (XRD). The morphology of samples after SPS was studied using field emission scanning electron microscopy (FE-SEM).

(Received September 10, 2013; accepted November 13, 2014)

**Keywords:** Mechanochemical process (MCP), TaC-TaB<sub>2</sub> composite, Spark plasma sintering, Density

## 1. Introduction

Hypersonic flights, re-entry vehicles, and propulsion applications all require new materials that can perform in oxidizing or corrosive atmospheres at temperatures in excess of 2000°C and sometimes over the course of a long working life. Ultra High Temperature Ceramics (UHTCs) are good candidates to fulfill these requirements [1]. Tantalum Carbide (TaC) is an ultra high-temperature ceramic (UHTCs) for high performance applications with a melting point in excess of 3900°C [2-4]. Unique combination of good chemical stability, good corrosion resistance, high modulus (537 GPa), high hardness (15–19 GPa) and other good mechanical properties make it a candidate material for rocket propulsion components [5-6] and many applications as high speed cutting tools, wear resistant parts, hard coating on hard metals and high temperature structural materials [2]. TaC has poor oxidation resistance. Since sintering typically occurs above 50% of the melting point, it is difficult to sinter TaC in conventional furnaces or through hot pressing. TaC has traditionally been difficult to densify due to its highly covalent bonding character and low self-diffusion coefficient. In view of the difficulty in densifying monolithic TaC, approaches to promote sintering have been explored by using mixed carbides and high pressure [7]. Another method for increasing the final density of sintered specimens is a reduction in the particle size of the powders. Research has shown that smaller powders produce a higher final density than coarser powders, particularly when decreasing from the micrometer to the nanometer scale [8]. This indicates that starting with nanoscale powders would be beneficial in

sintering a material like TaC, which is normally difficult to densify. Liu et al [9] have shown that initial particle size is essential to the final density of sintered TaC, with larger initial particle size indicating a lower final density, using a high heating rate that uses induction of electrical current to heat the die, rather than direct current flow through the die as in Spark sintering. Initial particle size and controlling final grain size while maintaining high density is key to successful applications of materials such as tantalum carbide. Spark plasma sintering (SPS), also known as the field assisted sintering technique, is becoming a widely used process in sintering research. SPS consists of conjoint application of high temperature, axial pressure and field-assisted sintering [10]. The field component is associated with an electric current passed through a powder specimen. SPS has advantages over conventional sintering or hot pressing, such as higher heating rates, shorter holding times, smaller post-processing grain sizes and denser final materials, many of which have been researched vigorously in the past few years [11]. The objective of this work is to study the synthesis of TaC-TaB<sub>2</sub> powder by additive B<sub>4</sub>C and densification of TaC-TaB<sub>2</sub> by spark plasma sintering.

## 2. Experimental Procedure

### 2.1 Powder preparation

The raw material characteristics are listed in table 1. The TaC content in the TaC powder was higher than 99%. The main impurities were 0.3 wt% Nb, 0.1 wt% Fe, 0.20 wt% O, 0.15 wt% free carbon, 0.05 wt% N, and Al, Ca, K,

Na, Ti with a total amount <0.05 wt%. The B<sub>4</sub>C was >95 wt% pure with major impurities of free carbon.

Table 1. Raw material characteristics.

Material	Purity	Particle size	Supplier
TaC	99%	1.25 μm	Ningxia Orient
B <sub>4</sub> C	>95 wt%	300 nm	Jingangzuan

Fig. 1,2 show X-ray diffraction patterns of the TaC and B<sub>4</sub>C raw materials.

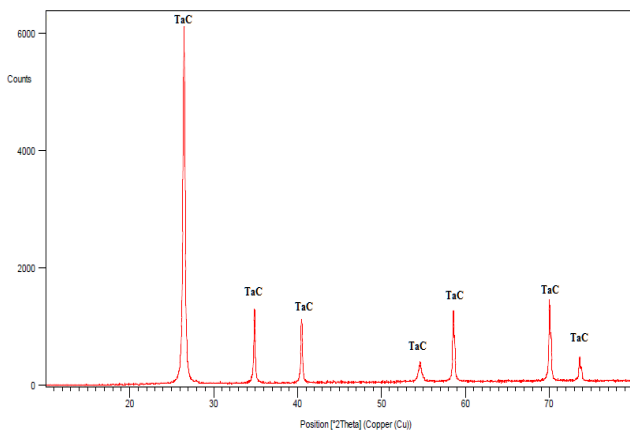


Fig. 1. X-ray pattern of raw TaC.

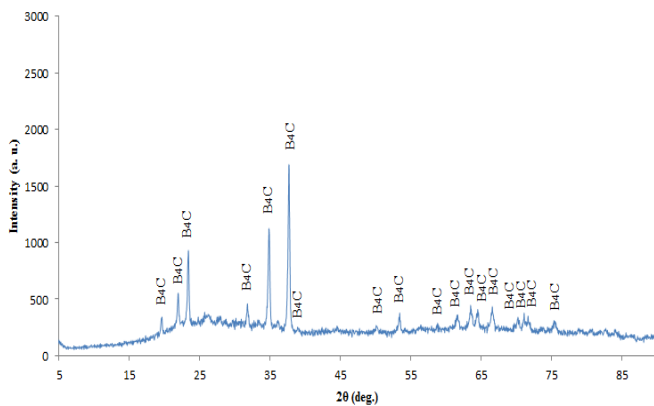


Fig. 2. X-ray pattern of raw B<sub>4</sub>C.

25g TaC and 2.0%Wt. B<sub>4</sub>C were mixed in a WC cylinder (250ml) using 150gr WC balls as mixing media. Ball milling of powder mixture was carried out in a planetary ball mill at room temperature in n-hexane and under argon atmosphere. The ball-to-powder weight ratio and the rotational speed of vial were 20:1 and 250 rpm, respectively for 0, 6 and 12 hours. The milling was interrupted at selected times and a small amount of powder was removed for further characterizations. Phase transformation during milling were determined by X-ray diffraction (XRD) in a Philips X'PERT MPD diffractometer using filtered Co K $\alpha$  radiation ( $\lambda = 0.178$  nm).

Crystallite size and internal strain of specimens ( $\mu$ ) were calculated from broadening of XRD peaks using the Williamson-Hall method [18], (eq1).

$$\beta \cos \theta = K\lambda / d + \mu \sin \theta \quad (1)$$

Where  $\theta$  is the Bragg diffraction angle,  $d$  is the average crystallite size,  $k$  is a constant (with a value of 0.9),  $\lambda$  is the wavelength of the radiation used, and  $\beta$  is the diffraction peak width at half maximum intensity.

## 2.2. Spark plasma sintering

Spark plasma sintering (SPS) was utilized to consolidate TaC-B<sub>4</sub>C and TaC-TaB<sub>2</sub> powders. SPS was carried out in Argon atmosphere at 1900°C. The heating rate of 100°Cmin<sup>-1</sup> was adopted to reach the maximum temperature with a hold time of 10min. SPS was carried out at 30MPa pressure. The powders were approximately 4–5mm thick and 15mm in diameter and were prepared using graphite dies and punches. Theoretical density for the sintered composites was determined by the law of mixtures. Bulk densities were measured by the Archimedes method. Relative density and open porosity was calculated. Phase compositions were analyzed by X-ray diffraction (XRD). The lattice parameter  $a$  for the cubic TaC<sub>y</sub> was calculated by refining the XRD. The C/Ta ratio in the TaC<sub>y</sub> was determined according to the equation  $a(y) = 4.3007 + 0.1563y$  [12]. That  $a$  is lattice parameter and  $y$  is C/Ta ratio. Microstructure and fracture surfaces were observed by field emission scanning electron microscopy (FE-SEM). The samples were sectioned, ground, and were polished to 1μm diamond finish.

## 3. Results and discussion

### 3.1. X-ray diffraction analysis synthesis powder

A commercial software program (HSC Chemistry) was used to identify the probable reaction using thermodynamic data. Fig.3 shows X-ray diffraction patterns of the TaC and TaC-TaB<sub>2</sub> powder after various milling time.

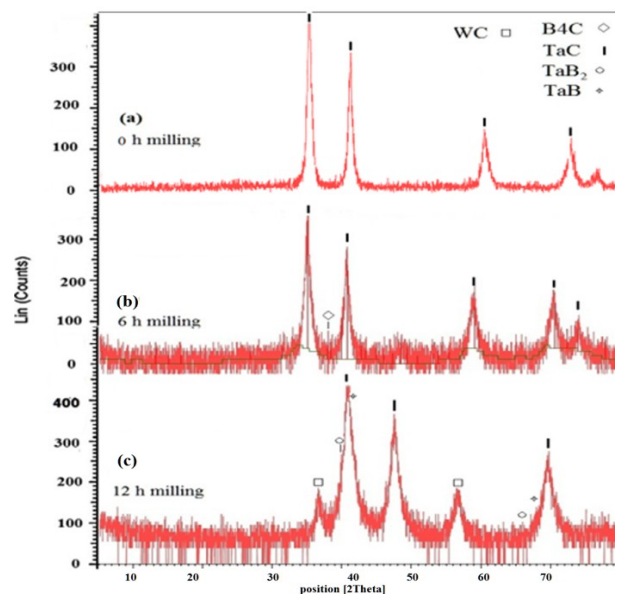


Fig. 3. XRD patterns of TaC-B<sub>4</sub>C powder after various milling time: (a) 0, (b) 6, and (c) 12 h.

Fig.(3-a) shows XRD pattern of raw tantalum carbide powder without milling. Fig.(3-b) shows the XRD results of the powders milled for 6 hours, TaB<sub>2</sub> phase unformed. The XRD analysis indicated that only TaB and TaB<sub>2</sub>, as presented in Fig. (3-c), were produced from the samples of their equivalent stoichiometries. Fig. (3-c) shows that the final products obtained from mechanochemical synthesis was free from three Ta-rich samples of Ta<sub>2</sub>B= 2:1, Ta<sub>3</sub>B<sub>2</sub>=3:2 and Ta<sub>3</sub>B<sub>4</sub>=3:4 contain a large amount of residual Ta. After 12h milling at fig (3-c) very small amount of TaB has been observed. No XRD peaks were observed for B<sub>4</sub>C, suggesting that a reaction had occurred in the system. Cup and balls of ball mill was made from WC so X-ray results show that increasing milling time up to 12 hours has caused a spike tungsten carbide. Fig(3-c). The grain size 'd' and strain 'μ' of TaC products during milling were measured by the Williamson–Hall method. The FWHM of the diffraction peak is wider with milling time due to the strain and the refinement of powder. The average grain sizes of the TaC calculated from the XRD data were about 801, 267 and 34 nm for the samples with milling times of 0, 6, and 12 h. According Eq.(1) and Williamson-Hall method calculation, internal strain and crystallite size of milled powder is shown in Fig.4. Internal strain of powders has increased with increasing milling time and crystallite size is reduced.

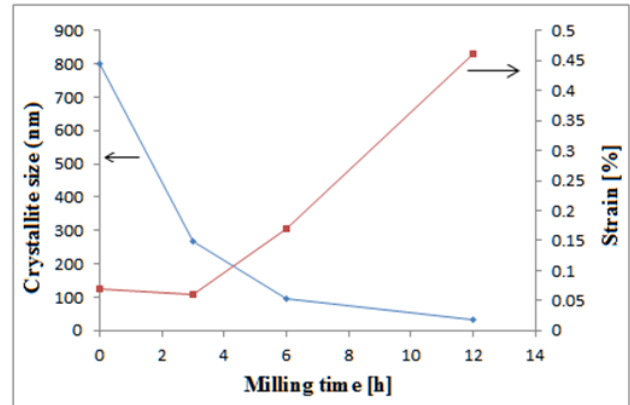


Fig. 4. Effect of milling time on the crystallite size and internal strain of powders.

### 3.2. X-ray diffraction analysis sintered samples

Typical XRD spectra, phase assembles and the calculated C/Ta ratios for cubic TaC<sub>y</sub> in the TaC/TaB<sub>2</sub> composites SPS were shown in Table 2. The ratio of C/Ta is confirmed by result of Hakett[13].

Table 2. Relative density, lattice parameter, phase assemble of the TaC/TaB<sub>2</sub> composites.

samples	Density (%)	Phase assemble	Lattice parameter	C/Ta in TaC <sub>y</sub>
A: 0 h	76	TaC <sub>y</sub> , TaB <sub>2</sub>	4.4446	0.92
B: 6 h	78	TaC <sub>y</sub> , TaB <sub>2</sub>	4.4571	1.0
C: 12 h	85	TaC <sub>y</sub> , TaB <sub>2</sub>	4.4712	1.09

Further, no XRD peaks were observed for B<sub>4</sub>C, suggesting that a reaction had occurred in the system. The change in standard Gibbs free energy ( $\Delta G^\circ$ ) indicated that Reaction (2) was favorable across the range of processing temperatures, which suggested that B<sub>4</sub>C reacted with TaC to form TaB<sub>2</sub> and C:



favorable across the processing temperature range. The XRD analysis and thermodynamic calculation were also consistent with the Ta-B-C phase diagram [14], which indicated that TaC is not chemically compatible with B<sub>4</sub>C. For the overall composition produced by adding relatively small amounts of B<sub>4</sub>C to TaC, the phase diagram indicated that TaB<sub>2</sub> and C were stable with TaC.

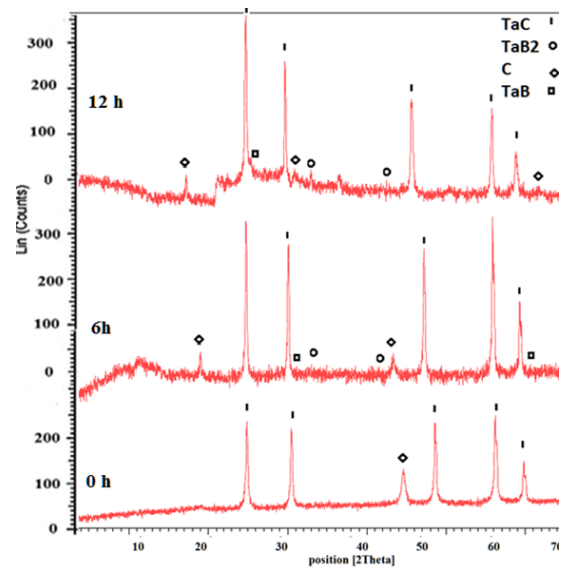


Fig. 5. XRD patterns of TaC-TaB<sub>2</sub> composites sintered by SPS. Composite powders after various milling time: (a) 12 h, (b) 6, and (c) 0 h.

Analysis of the XRD patterns (Fig. 5) showed a progressive increase in the amount of the TaB<sub>2</sub> phase formed during SPS. The amounts of TaB<sub>2</sub> formed could be as high as 14 wt.% for a B<sub>4</sub>C addition of 2 wt.%, if all of the B<sub>4</sub>C were consumed by Reaction (2). The relative densities of the samples were significantly improved by increasing milling time. The milling time increase up to 12 h (Table 2). The lattice parameter of TaC powder obtained from 0, 6 and 12 h milling is calculated by Nelson–Riley method from the XRD analysis. The result shows that lattice parameter increases by increasing milling time. By increasing milling time, B<sub>4</sub>C is decomposed and TaB<sub>2</sub> according Fig.4 is formed. Table 2 shows C/Ta ratios for the cubic TaC<sub>y</sub> in different samples. The C/Ta values increased with milling time of raw powder samples [16]. Fig. 6 shows the free energy of the reaction as a function of temperature as calculated from Thermochemical database of software HSC. It is observed that the free energy of the reaction is negative (−48.0 kJ mol<sup>−1</sup>) at the SPS temperatures of 1900°C. This indicates that not only the reaction is thermodynamically feasible but is also exothermic and will help in further consolidation [17].

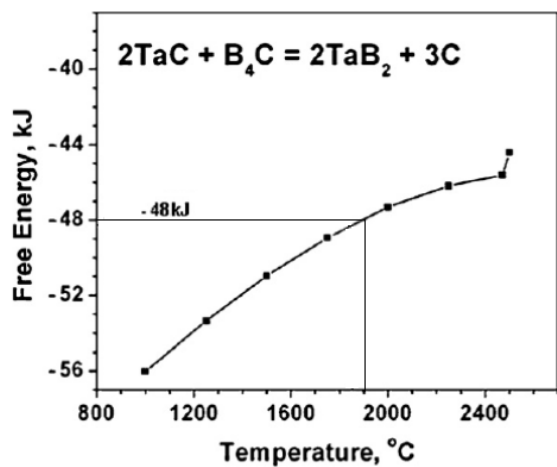


Fig. 6. Variation of Free energy of TaB<sub>2</sub> formation by reaction between TaC and B<sub>4</sub>C as a function of temperature.

### 3.3. Densification

The relative densities of TaC-TaB<sub>2</sub> ceramics sintered using different powders at the given temperature are shown in Fig. 7. After sintering at 1900°C and 30 Mpa pressure for 10 min, the relative density of sample A is still as low as 76%, indicating poor sinterability of powder A. The relative densities of TaC ceramics prepared using powder B and C are 78% and 85% (Table 2).

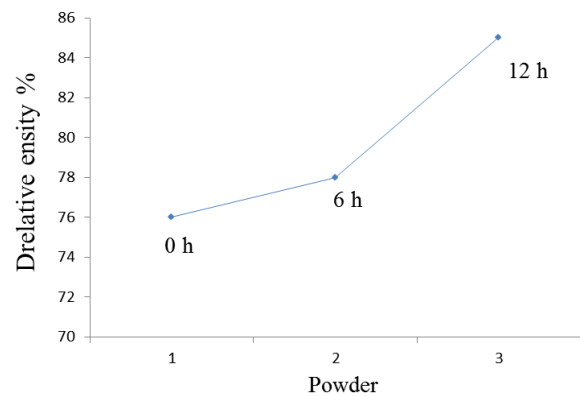


Fig. 7. Relative density of the sintered ceramics as a function of particle size of powder.

Even after sintering at 1900°C, the relative density of sample A is still 76%. The particle size of powder A was 801 nm. The microstructures of the sample were illustrated in Fig. 8. This figure shows that the fracture surface of the dense TaC ceramics prepared using powder A. During sintering sample by using powder A, fast grain growth occurred, which entrapped big pores into the TaC grains, as shown in Figs. 8(a) [15]. This figure shows grain structure with a large grain size of about 4–6 μm. The pores between the particles can be clearly seen in Fig. 8(b).

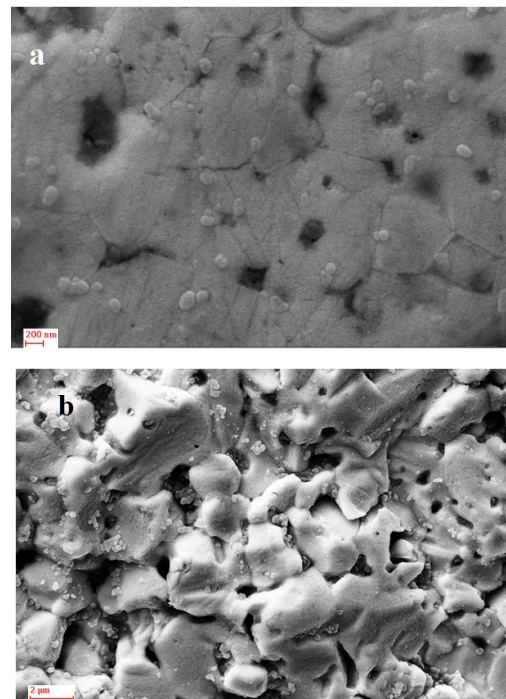


Fig. 8. FE-SEM morphologies of sample A. (a), (b) fracture surfaces of sample A.

The ceramics prepared using powder B at given temperature show fine microstructures (see Fig. 9). The particle size of powder B was 267 nm. This figure shows fine grain structure with a grain size of about 1–3 μm. The residual pores in these samples are smaller than those of sample A.

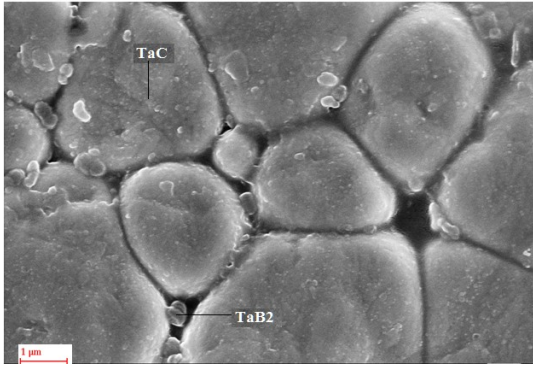


Fig. 9. FESEM morphologies of the fracture surfaces of sample B.

Fig. 9 shows that there are phases present at the grain boundaries of TaC which could be TaB<sub>2</sub> phase mixtures. The TaB<sub>2</sub> present at grain boundaries leads to pinning of the grain boundaries and arrests grain growth. EDX analysis of sample B is shown in Fig. 10.

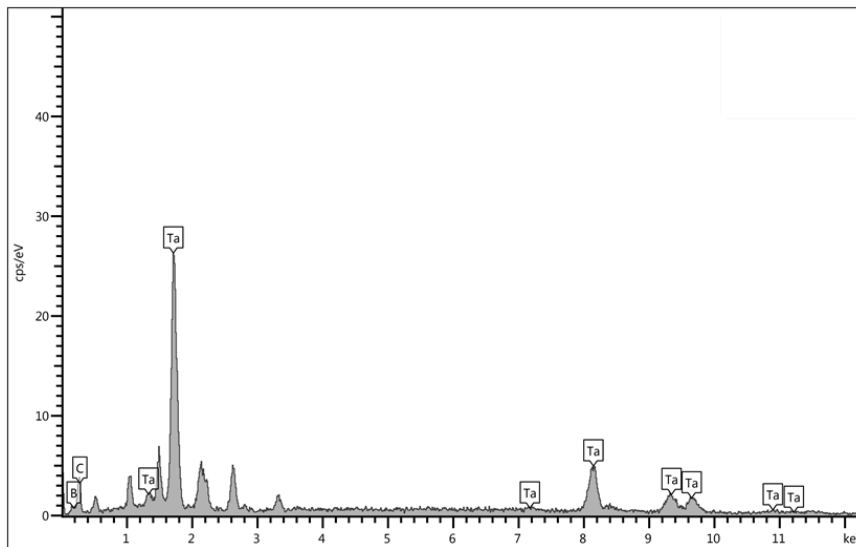


Fig. 10. EDX analysis of sample B. (Fig. 6).

Fig. 11 shows the surface of sample C after sintering. The average grain sizes of sample C after SPS were maintained at small values of about 1 μm. The relative density of this sample was 85% and in this figure there are some pores after sintering. Comparing the relative densities and microstructures of samples A, B and C, all the samples show fine microstructures, but sample C has the highest relative density among them (85%).

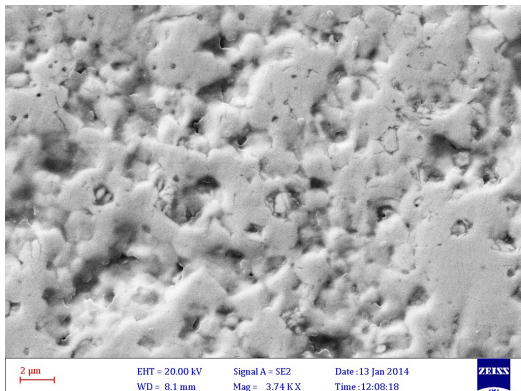


Fig. 11. FE-SEM morphologies of the fracture surfaces of sample C.

#### 4. Conclusion

Using fine TaC powder with narrow particle-size distribution, monolithic TaC ceramics with a relative density of 85% was obtained by spark plasma sintering at 1900°C with adding 2wt.% B<sub>4</sub>C as an additive. With decreasing particle size of powders, samples after sintering had fine grain structure and density of this sample was more than the other samples. Addition of B<sub>4</sub>C has dual advantages viz. (i) as a sintering aid and (ii) grain growth inhibitor. XRD patterns and FE-SEM images suggested that TaC reacted with B<sub>4</sub>C leading to formation of TaB<sub>2</sub>. The TaB<sub>2</sub> present at grain boundaries leads to pinning of the grain boundaries and arrests grain growth.

#### Acknowledgement

The authors are indebted to the material department in Malek-e-ashtar University of Technology, that supplied the raw materials for the development of this research and to the building and construction department of Standard Research Institute for its equipment support.

## References

- [1] J.F. Justin, A. Jankowiak, *Theonera journal of aerospace lab.* **3**, 1 (2011).
- [2] T.H. Squire, J. Marschall, *J. European Ceramic Society.* **30**, 2239 (2010).
- [3] D. Hwan Kwon, S. H. Hong, B. K. Kim, Fabrication of ultrafine TaC powders by mechano-chemical process, *J. Materials Letters.* **58** (2004) 3863– 3867.
- [4] F. Monteverde, A. Bellosi, L. Scatteia, *J. Materials Science and Engineering.* **485**, 415 (2008).
- [5] X. Zhang, G. E. Hilmas, W. G. Fahrenholtz, *J. Materials Science and Engineering.* **501**, 37 (2009).
- [6] G. Hagemann, H. Immich, T. V. Nguyen, E. Gennady, *J. Propulsion and powder.* **14** (1998).
- [7] X. Zhang, G. E. Hilmas, W. G. Fahrenholtz, *J. Am. Ceram. Soc.* **90**, 393 (2007).
- [8] Z. Shen, M. Johnsson, Z. Zhao, M. Nygren, *J. Am. Ceram. Soc.* **85**, 1921 (2002).
- [9] J. X. Liu, Y. M. Kan, G. J. Zhang, *J. Am. Ceram. Soc.* **93**, 370 (2010).
- [10] Z. Shen, M. Johnsson, Z. Zhao, M. Nygren, *J. Am. Ceram. Soc.* **85**, 1921 (2002).
- [11] E. Khaleghi, Y. S. Lin, M. A. Meyers, E. A. Olevsky, *J. ScriptaMateriali.* **63**, 577 (2010).
- [12] Bowman AL, *J Phys Chem.* **65**, 1596 (1961).
- [13] K. R. Hackett, Phase constitution and mechanical properties of carbides in the Ta - C system, The University of Utah, May 2009.
- [14] A. E. McHale, System B–Ta–C. Isothermal Section at 1750°C. Phase Equilibria Diagrams, Phase Diagrams for Ceramists, Volume X Borides, Carbides, and Nitrides. The American Ceramic Society, Westerville, OH, 1994.
- [15] L. Liu, H. Liu, F. Ye, Z. Zhang, Y. Zhou, *J. Ceramics International.* **38**, 4707 (2012).
- [16] L. Liu, F. Ye, Y. Zhou, Z. Zhang, *J. Am. Ceram. Soc.* **93**, 2945 (2010).
- [17] S. R. Bakshi, V. Musaramthota, D. Lahiri, V. Singh, S. Seal, A. Agarwal, *Materials Science and Engineering A.* **528** 1287 (2011).
- [18] G. K. Williamson, W. Hall, *J. Acta Metall.* **1**, 22 (1953).

\*Corresponding author: beh\_mehdikhani@yahoo.com